Intraprocedural Imaging of Left Atrial and Pulmonary Vein Anatomy for Atrial Fibrillation Ablation

R Chan[1], A Thiagalingam[2], A d'Avila[2], I Ho[2],
V Reddy[2], R Manzke[1]

[1]Philips Research North America, Briarcliff Manor, NY, USA
[2]Massachusetts General Hospital, Boston, MA, USA

Abstract

Image guidance facilitates catheter-based ablation of atrial fibrillation. Preprocedural magnetic resonance (MR) or computed tomographic (CT) imaging of the left atrium (LA) and pulmonary veins (PV) has been used to derive essential information about cardiac anatomy, however, significant changes in morphology can occur between preprocedural imaging and the actual intervention. The two procedures can be separated in time by days or even weeks, during which changes in volume status and other physiological factors can occur. We present and validate an intraprocedural imaging method based on contrast-enhanced 3D rotational X-ray angiography (3DRA) which allows for near-real-time 3D characterization of LA/PV anatomy with good accuracy and reproducibility.

1. Introduction

Atrial fibrillation affects more than 2.5 million people in the US annually and is associated with elevated stroke risk and morbidity. There has been rapid growth of $\sim$27% per year in AF interventional procedures which target the termination of arrhythmias arising from ectopic sites in the left atrium (LA) and pulmonary veins (PVs). Catheter-based radiofrequency ablation has become the dominant treatment, but remains technically challenging and time-consuming to perform, due to the need for accurate placement of ablation lesions in complex patterns for electrical isolation [1].

To address the need for reducing intervention times, minimizing radiation dose, increasing clinical efficacy and maximizing case throughput, a number of different guidance strategies have been deployed, including electroanatomical mapping (EAM) and pre-procedural imaging with cardiac MRI or CT [1, 2, 3, 4]. EAM is a tedious procedure in which a sparse number of cardiac surface points is used to produce coarse surface visualization to aid catheter navigation. MRI and CT provide detailed 3D representations of the LA/PV anatomy, however, the time between pre-procedural imaging and intervention can vary from days to weeks, leading to anatomical variations due to patient position, volume status and other physiological factors.

We present and validate an intraprocedural imaging technique based on rotational X-ray imaging that allows for near-real-time 3D characterization of cardiac anatomy.

2. Methods

Intra-procedural, contrast-enhanced rotational X-ray imaging was performed in 42 patients using a Philips Allura FD10 flat-detector system. Following cardiac isocentering, the X-ray C-arm was rotated in propeller mode over a 220° arc around each subject. For each rotation, 120 cone-beam projections were captured at 30Hz and ungated volumetric reconstruction was performed using a standard approximate Feldkamp (FDK) backprojection algorithm on the system workstation [5]. For cone-beam projections, $p(\beta,\mu,\nu)$, rotational angle β and detector coordinates (μ,ν) , the reconstruction equations used were:

$$w(\mu,\nu) = \frac{\overline{SO}}{\sqrt{\overline{SO}^2+\mu^2+\nu^2}}\,, \quad (1)$$

$$p^f(\beta,\mu,\nu) = \{w(\mu,\nu)\cdot p(\beta,\mu,\nu)\} * h(\mu)\,, \quad (2)$$

$$f(\vec{x}) = \int_0^{2\pi} \frac{\overline{SO}^2}{U^2(x,y,\beta)} p^f(\beta,\mu(x,y,\beta),\nu(\vec{x},\beta))d\beta\,, \quad (3)$$

In these equations, the distance from source to the detector is $\overline{SO}$, $h(\cdot)$ is the ramp filter kernel, $\vec{x}=(x,y,z)^T$ is the voxel coordinate and $f(\cdot)$ is the object function. $w(\mu,\nu)$ specifies the cone-angle dependent pre-weighting and $U(\cdot)$ is the voxel-dependent weighting of the FDK algorithm. The acquisition workflow used clinically is illustrated in Figure 1. A 60mL contrast bolus was injected at 20mLs^{-1} into each of the left and right pulmonary arteries (PA). The total breath-hold time was $\sim$10s, spanning contrast injection (3s), pulmonary transit delay (3-4s) and image acqui-

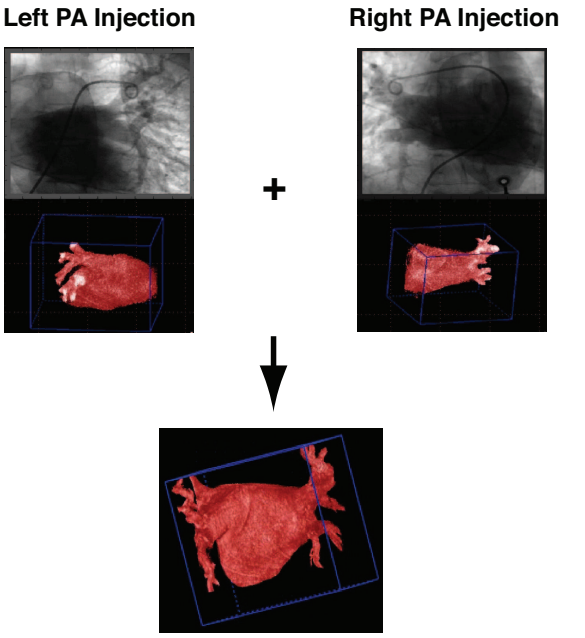

Figure 1. Clinical workflow. Rotational datasets were acquired from selective injections into the left and then right pulmonary arteries. Volumetric reconstruction from each rotational acquisition was performed and the results were fused together using rigid-body registration of the spine which appears in both volumes. Single injections were also used for LA/PV chambers that were small enough to fit entirely within the FD10 field-of-view.

sition (4s). The reconstructed LA/PV volumes were fused together based on rigid-body registration of the spine in each acquisition. For patients with cardiac anatomy small enough to fit fully within the FD10 field-of-view, a single injection was used.

Imaging accuracy and reproducibility was assessed by independent expert reviewers. PV ostial diameters were measured from the 3DRA volume visualizations and were compared with those from reference cardiac MR/CT imaging. Analysis of the measurement differences was performed with the Kruskal-Wallis test for statistically significant differences between intraprocedural & preprocedural imaging and between observers.

3. Results

Figure 2 illustrates examples of intraprocedural 3DRA imaging. All 42 imaging results were assessed by two independent expert reviewers and classified into non-diagnostic (28%), useful (55%) and optimal (17%) studies. Non-diagnostic studies did not show adequate anatomical detail for ablation guidance, whereas useful studies showed the necessary anatomical information. Optimal

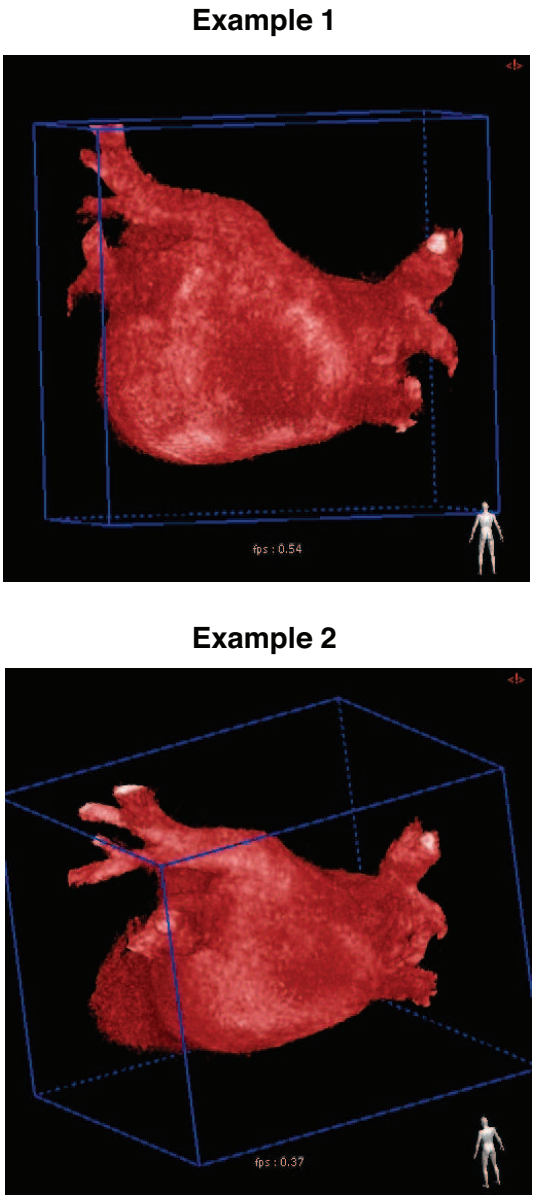

Figure 2. Volumetric reconstructions from 2 sample studies. The level of anatomical detail compared favorably with that from pre-procedural imaging.

studies showed not only the necessary anatomy, but also demonstrated excellent image quality. The left atrial appendage was visualized in 57% of cases. Separate and blinded measurements of ostial diameters in preprocedural and intraprocedural volumes resulted in mean absolute differences of 2.7±2.3 mm for the left-superior PV, 2.2±1.8 mm for the left-inferior PV, 2.4±2.2 mm for the right-superior PV and 2.2±2.3mm for the right-inferior PV. The LSPV was measurable in 85.7%, LIPV in 79.6%, RSPV in 70.2% and RIPV in 73.8%. In contrast, “”side-

Fluoroscopic overlay of LA/PV anatomy

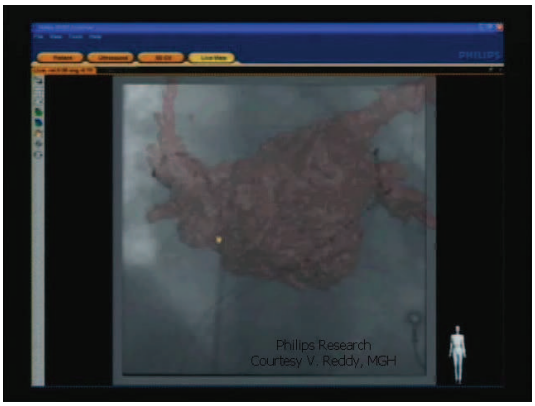

Electroanatomical point overlay

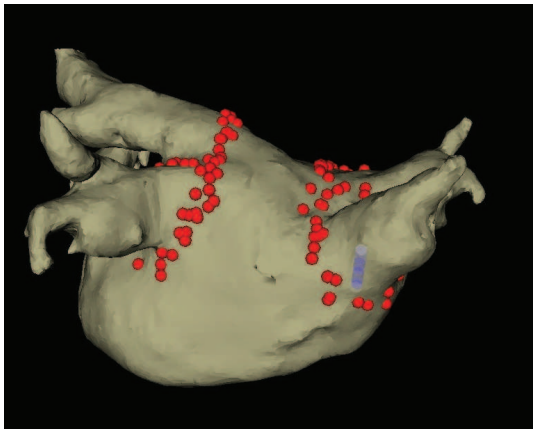

Figure 3. Intraprocedural overlay of LA/PV anatomy on live fluoroscopy to aid navigation of catheters visible in fluoroscopy is shown in the top panel, whereas fusion of electroanatomical mapping points with 3DRA-derived LA/PV anatomy is shown in the bottom panel.

by-side" measurements of preprocedural and intraprocedural datasets resulted in 1.8±1.4 mm for the LSPV, 1.7±1.5 mm for the LIPV, 1.5±1.1 mm for the RSPV and 1.7±1.2 mm for the RIPV. An average diameter difference of less than 2-3mm was observed, and this is in the order of a typical ablation lesion size. No statistically significant differences were found in measurements between modalities and between expert reviewers. Figure 3 illustrates intraprocedural use of the 3DRA-derived LA/PV surfaces obtained for each of our clinical studies. Our anatomical models were used as graphical overlays with live X-ray fluoroscopy to aid in catheter navigation relative to anatomical features. Our models were also fused with electroanatomical mapping data for visualization of catheter position, ablation points and cardiac anatomy within the EAM software.

4. Discussion and conclusions

Intraprocedural CT-like volumetric imaging of LA/PV anatomy for AF ablation guidance is rapid, clinically-feasible, and yields anatomical detail that shows good agreement with preprocedurally-acquired cardiac MR or CT datasets. Further work is underway to reduce the percentage of non-diagnostic studies, to incorporate motion-compensation into the reconstruction process, and to obtain LA/PV surface segmentations that are robust to imaging artifacts/noise.

Acknowledgements

This work was supported in part by an NIH K23 award (HL68064) to Dr. Reddy and by Philips Research; Dr. Thiagalingam is supported by the NHF/NHMRC Neil Hamilton Fairley Training Fellowship (NHMRC Grant ID: 408106). The authors also thank Andrew H. Locke for help in experimental setup and data acquisition.

References

[1] Haissaguerre M, Jais P, Shah DC, Takahashi A, Hocini M, Quiniou G, Garrigue S, Mouroux AL, Metayer PL, Clementy J. Spontaneous initiation of atrial fibrillation by ectopic beats originating in the pulmonary veins. New England Journal of Medicine 1998;339:659 – 666.

[2] Pappone C, Oreto G, Rosanio S, et al. Atrial electroanatomic remodeling after circumferential radiogrequency pulmonary vein ablation: efficacy of an anatomic approach in a large cohort of patients with atrial fibrilation. Circulation 2001; 104:2539 – 2544.

[3] Reddy VY, Malchano ZJ, Holmvang G, Schmidt EJ, dAvila A, Houghtaling C, Chan RC, Ruskin JN. Integration of cardiac magnetic resonance imaging with three-dimensional electroanatomic mapping to guide left ventricular catheter manipulation. Journal of the American College of Cardiology 2004;44(1):2202 – 2213.

[4] Mikaelian BJ, Malchano ZJ, Neuzil P, Weichet J, Doshi SK, Ruskin JN, Reddy VY. Integration of three-dimensional cardiac computed tomography images with real-time electroanatomic mapping to guide catheter ablation of atrial fibrillation. Circulation 2005;112:35 – 36.

[5] Feldkamp LA, Davis LC, Kress JW. Practical cone-beam algorithm. Journal of the Optical Society of America 1984; A6:612 – 619.

Address for correspondence:

Raymond C. Chan
Philips Research North America
345 Scarborough Road
Briarcliff Manor, NY, 10510
ray.chan@philips.com